24th COBEM - 2017

24th ABCM International Congress of Mechanical Engineering
December 3-8, 2017, Curitiba, PR, Brazil

COBEM-2017-0405
MECHANICAL EFFICIENCY DETERMINATION OF A DEDICATED HYBRID TRANSMISSION USING GRAPH AND SCREW THEORIES: A CASE STUDY

Marina Baldissera de Souza
Rodrigo de Souza Vieira
Daniel Martins
Universidade Federal de Santa Catarina, Departamento de Engenharia Mecânica, Centro Tecnológico, Campus Universitário - Trindade, CEP: 88.040-900, Florianópolis/SC - Brasil
marina.bs@posgrad.ufsc.br – rodrigo.vieira@ufsc.br – daniel.martins@ufsc.br

Humberto Reder Cazangi
Instituto Federal de Santa Catarina, Campus Florianópolis, Departamento Acadêmico de Metal Mecânica, Av. Mauro Ramos, 950, CEP: 88.020-300, Florianópolis/SC - Brasil
humbertoreder@ifsc.edu.br

Luís Paulo Laus
Universidade Tecnológica Federal do Paraná, Departamento Acadêmico de Mecânica, Av. 7 de Setembro, 3165, CEP: 80.230-901, Curitiba/PR - Brasil
laus@utfpr.edu.br

Abstract. *Hybridization is a promising solution to reduce regulated emissions without compromising fuel consumption, what makes the development of transmission systems for Hybrid Electric Vehicles a relevant and prolific study field. Inside this scenario, one new transmission category emerges: the Dedicated Hybrid Transmission (DHT), which includes transmission systems that use at least two sources of propulsion, an internal combustion engine (ICE) and at least one electric motor (EM), and whose functionality depends on both propulsion sources. One important aspect to be studied is the gear trains' mechanical efficiency of DHTs. In this paper, a DHT available on the market was selected as a case study. In order to determine the gear set efficiency for each driving mode, graph and screw theories and the Kirchhoff laws were applied, through an electromechanical analogy where the friction losses are taken into account by considering them analogues of the electrical resistance. The objective is to determine the most efficient driving mode and to identify the features in the transmission's topology which compromise the global efficiency.*

Keywords: *Efficiency, Automotive transmission, Hybrid electric vehicles, Graph and screw theories, Electromechanical analogy*

1. INTRODUCTION

Reducing regulated emissions without compromising fuel consumption is a challenge faced by the automotive industry. Hybridization is a promising solution, what makes the development of transmission systems for Hybrid Electric Vehicles (HEV) a relevant and prolific study field. On this domain, a new transmission category emerges: the Dedicated Hybrid Transmission (DHT), which comprises drivetrains that use at least two sources of propulsion, an internal combustion engine (ICE) and at least one electric motor (EM) fully integrated with the transmission, whose functionality depends on both propulsion sources. One important aspect to be studied is the DHT gear trains mechanical efficiency, whose value has a direct impact on fuel economy (Moskalik *et al.*, 2016). Experimental methods aiming to estimate automotive transmissions' performance are available in the literature. Irimescu *et al.* (2011) developed a model for calculating the overall transmission efficiency of passenger cars by employing a chassis dynamometer. Mantriota (2002) measured the performance of an infinitely variable transmission using a special test rig and compared the results with a theoretical model. Notwithstanding the importance of having empirical values, it is not viable to execute experimental procedures in the phase of project of a drivetrain. Therefore, there is a need of realistic simulation tools to predict power losses. Changenet *et al.* (2006) presented a model which estimates the power losses in a six-speed manual gearbox, based on the first principle of Thermodynamics for transient conditions. Hsieh and Tsai (1998) developed a method to estimate

the efficiency of automatic transmission mechanisms according to the clutching sequences, allowing to appoint the most efficient one. However, their method is limited to the presence of coaxial links.

In this paper, a commercial DHT was chosen as a case study, and the mechanical efficiency of each driving mode is determined through electromechanical analogy, based on graph and screw theories, which enable to consider the friction losses as analogous to the electrical resistance. This method has no restrictions regarding the transmission's geometry and axes' relative positions. It is established which DHT's driving mode presents the best performance, and the aspects in the transmission's topology that affect the global efficiency are identified as well. Section 2. introduces necessary concepts in the application of the electromechanical analogy, presenting in Section 2.1 and Section 2.2 the adaptation of Kirchhoff's Voltage and Current Laws, respectively. In Section 2.3, it is explained how the overall eficiency and the efficiency of a gear pair are calculated. Section 2.4 presents how the loss sources are added to the simulation. In Section 3., the model of the DHT used in the simulations is described and simplifying assumptions are listed. Section 4. presents the simulations' results and a brief analysis of the efficiency values besides the sensitivity of each driving mode. Finally, in Section 5., final considerations and suggestions of future contributions to this research are made.

2. ELECTROMECHANICAL ANALOGY THROUGH GRAPH AND SCREW THEORIES

This section briefly introduces some base concepts for the application of the electromechanical analogy applied in this paper. Interested readers should refer to the work of Cazangi (2008) and Laus *et al.* (2012).

Davies (1981) presented an equivalent of the Kirchhoff voltage and current laws for a network of links (bodies) and couplings, based on graph and screw thories. In this adaptation, a multibody system is represented by a graph, whose edge variables model the actions transmitted by the coupling and the motions allowed by it. The edge variables modeling the actions are analogous to the electric current (*through variable*) as those that modeling the motions are analogous to the voltage (*across variable*). By using these analogies, the motion and the action analyses of a mechanism may be done independently.

From the graph theory application into mechanism's analysis, the graph's nodes represent the links and its edges, the couplings. ν is the number of fundamental circuits of a graph and it is determined by $\nu = j - n + 1$, where j is the number of couplings of the mechanism and n, the number of links. The number of fundamental cutsets κ of a graph is the number of links diminished by one ($\kappa = n - 1$). The fundamental circuits and the fundamental cutsets of a graph can be mathematically represented by the *fundamental circuit matrix* $[B_M]_{\nu \times F}$ and *fundamental cutset matrix* $[Q_A]_{\kappa \times C}$. F is the *gross degree of freedom* of a mechanism, which is the sum of all independent unitary motions f allowed by each coupling. C is the *gross degree of constraint*, determined by the sum of all independent unitary constraints c of each coupling and the constraints representing external efforts acting on the mechanism.

A *screw* \$ is a geometrical element that can represent mechanical quantities. It is defined by a straight line (instantaneous screw axis - ISA) and an associated pitch h, which has unit of length. A *normalised screw* $\hat{\$}$ has a unitary vector standing for its defining straight line (Cazangi, 2008). The number of non-null elements of the screw defines the order of the system λ, which is the dimension of the space where the coupling is represented and it can be estimated by two dual terms f and c, being given by $\lambda = f + c$. The denomination of the screws and the arrangement of its elements depend on the kind of analysis to be done.

2.1 Motion analysis

In the **motion analysis**, the instantaneous state of motion of a rigid body, relative to an inertial system with coordinates O_{xyz}, can be described by a screw called *twist* $\$^m$, which is a combination of an angular velocity ω around the ISA and a linear velocity τ on the same axis. The twist's pitch is defined as $h = \tau/\omega$.

The twist is composed by an angular velocity vector $\vec{\omega} = \{r, s, t\}$ and a linear velocity vector $\vec{V_P} = \{u, v, w\}$, quantifying the velocity of a rigid body's point instantaneously at the origin of O_{xyz}. The twist is organized in axis formation:

$$\$^m = \begin{pmatrix} \vec{\omega} \\ - - - \\ \vec{V_P} \end{pmatrix} = \begin{pmatrix} r \\ s \\ t \\ - - - \\ u \\ v \\ w \end{pmatrix} = \begin{pmatrix} \vec{\omega} \\ - - - - - - - - - \\ \vec{S_0} \times \vec{\omega} + h\vec{\omega} \end{pmatrix} = |\vec{\omega}| \begin{pmatrix} \vec{S^M} \\ - - - - - - - - - - - \\ \vec{S_0} \times \vec{S^M} + h\vec{S^M} \end{pmatrix} \tag{1}$$

$\vec{S^M}$ is the unit vector defining the direction of the twist's ISA and $\vec{S_0}$ is the position vector of any point on the twist's axis regarding O_{xyz}. $\vec{V_P}$ is the result of the addition of the parallel velocity to the twist's ISA, represented by $h\vec{\omega}$, and the normal velocity to the twist's instantaneous axis, represented by $\vec{S_0} \times \vec{\omega}$. A pure angular velocity has $h = 0$ and a pure linear velocity has $h \to \infty$.

The magnitude φ^m of the twist is given by the angular velocity magnitude $|\vec{\omega}| = \sqrt{r^2+s^2+t^2}$ when $h \neq \infty$. Otherwise, φ^m is given by the linear velocity magnitude $\left|\vec{V_P}\right| = \sqrt{u^2+v^2+w^2}$ when $h \to \infty$. φ^m is used to normalise the twist: $\$^m = \varphi^m \hat{\$}^m$ (Cazangi, 2008).

All the twists of a mechanism are disposed side by side to form the *motion matrix* $[M_D]_{\lambda \times F} = \left[\begin{array}{cccc} \$_a^m & \$_b^m & \cdots & \$_F^m \end{array} \right]$.

The *unit motion matrix* $[\hat{M}_D]_{\lambda \times F}$ is composed by the normalised twists: $[\hat{M}_D]_{\lambda \times F} = \left[\begin{array}{cccc} \hat{\$}_a^m & \hat{\$}_b^m & \cdots & \hat{\$}_F^m \end{array} \right]$.

The vector $\{\vec{\psi}\}_{F \times 1}$ contains the magnitudes of the twists: $\{\vec{\psi}\}_{F \times 1} = \left\{ \begin{array}{cccc} \varphi_a^m & \varphi_b^m & \cdots & \varphi_F^m \end{array} \right\}^T$.

The motion analysis is done through the adaptation of the Kirchhoff's Voltage Law, establishing relations among the motions of the couplings belonging to the same circuit. The Kirchhoff's Voltage Law states that algebraic sum of the electrical potential differences around any closed network is zero. Analogously, Davies (1981) states that the algebraic sum of the twists around any circuit is zero. Each one of the λ components of the twists belonging to a circuit must have its sum equals to zero, this is mathematically translated by doing ν times the product between $[\hat{M}_D]_{\lambda \times F}$ and a diagonal matrix whose main diagonal is composed by the elements of each row of $[B_M]_{\nu \times F}$. That operation results in the the *network unit motion matrix* $[\hat{M}_N]_{\lambda\nu \times F}$. Multiplying this matrix by $\{\vec{\psi}\}_{F \times 1}$ and forcing to zero, gives the system of equations of the motion analysis. The vector $\{\vec{\psi}\}_{F \times 1}$ contains the unknown variables of the equation system, and this statement can be mathematically modeled by:

$$[\hat{M}_N]_{\lambda.\nu \times F} \{\vec{\psi}\}_{F \times 1} = \{\vec{0}\}_{\lambda.\nu \times 1} \tag{2}$$

The F unknown variables related by the $\lambda.\nu$ equations can be written as function of a subset of F_N known variables, which are called *primary variables*. F_N is the *net degree of freedom* and it is determined by the difference between F and the rank m of the matrix $[\hat{M}_N]_{\lambda.\nu \times F}$:

$$F_N = F - m \tag{3}$$

The value of F_N establishes the number of variables belonging to $\{\vec{\psi}\}_{F \times 1}$ that must be imposed in order to solve the system of equations, i.e., to determine the values of the remaining m unkown variables, called *secondary variables*. Thus the terms of Eq. (2) can be rearranged as:

$$\{\vec{\psi}_S\}_{m \times 1} = -[\hat{M}_{NS}]^{-1}_{m \times m} [\hat{M}_{NP}]_{m \times F_N} \{\vec{\psi}_P\}_{F_N \times 1} \tag{4}$$

The vector $\{\vec{\psi}\}_{F \times 1}$ is updated with the primary variables and the solution of Eq. (4), then pre-multiplied by $[\hat{M}_D]_{\lambda \times F}$, resulting in the motion matrix $[M]_{\lambda \times F}$:

$$[M]_{\lambda \times F} = [\hat{M}_D]_{\lambda \times F} \{\vec{\psi}\}_{F \times 1} \tag{5}$$

The condensed version of the motion matrix is obtained by adding together the columns related to the same coupling, resulting in a matrix with dimensions $\lambda \times j$, where j is the number of couplings of the mechanism analysed.

2.2 Action analysis

In the **action analysis**, the action state of a rigid body, relative to an inertial system with coordinates O_{xyz}, can be described by a screw called *wrench* $\$^a$, which is a combination of a line vector comprising the component of resultant force $\vec{F}_R$, whose line of action defines the screw axis, and a free vector comprising a torque $\vec{T}$, parallel to the same axis. The wrench pitch is defined as $\vec{T} = h\vec{F}_R$.

The wrench is composed by a moment vector $\vec{T}_P = \{R, S, T\}$, which acts on a rigid body's point instantaneously at the origin of O_{xyz}, and a force vector $\vec{F}_R = \{U, V, W\}$. The wrench is organized in ray formation:

$$\$^a = \begin{pmatrix} \vec{T}_P \\ - - - \\ \vec{F}_R \end{pmatrix} = \begin{pmatrix} R \\ S \\ T \\ - \; \bar{U} \; - \\ V \\ W \end{pmatrix} = \begin{pmatrix} \vec{S_0} \times \vec{F}_R + h\vec{F}_R \\ - - - - - - - - - - - \\ \vec{F}_R \end{pmatrix} = \left|\vec{F}_R\right| \begin{pmatrix} \vec{S_0} \times \vec{S}^A + h\vec{S}^A \\ - - - - - - - - - - - \\ \vec{S}^A \end{pmatrix} \tag{6}$$

$\vec{S}^A$ is the unit vector defining the direction of the wrench's ISA and $\vec{S_0}$ is the position vector of any point on the wrench's axis in relation to O_{xyz}. A pure force has $h = 0$ and a pure torque has $h \to \infty$.

The magnitude φ^a of the wrench is given by the force magnitude $\left|\vec{F_R}\right| = \sqrt{U^2+V^2+W^2}$ when $h \neq \infty$. Otherwise, φ^a is given by the torque magnitude $\left|\vec{T_P}\right| = \sqrt{R^2+S^2+T^2}$ when $h \to \infty$. φ^a is used to normalise the wrench: $\$^a = \varphi^a \hat{\$}^a$ (Cazangi, 2008).

All the wrenches of a mechanism are disposed side by side to form the *action matrix* $[A_D]_{\lambda\times C} = \left[\begin{array}{cccc} \$_a^a & \$_b^a & \cdots & \$_C^a \end{array} \right]$

The *unit action matrix* $[\hat{A}_D]_{\lambda\times C}$ is composed by the normalised wrenches: $[\hat{A}_D]_{\lambda\times C} = \left[\begin{array}{cccc} \hat{\$}_a^a & \hat{\$}_b^a & \cdots & \hat{\$}_C^a \end{array} \right]$.

And the vector $\{\vec{\Psi}\}_{C\times 1}$ contains the magnitudes of the wrenches: $\{\vec{\Psi}\}_{C\times 1} = \left\{ \begin{array}{cccc} \varphi_a^a & \varphi_b^a & \cdots & \varphi_C^a \end{array} \right\}^T$.

The action analysis is done through the adaptation of the Kirchhoff's Current Law, establishing relations among the actions belonging to the same cutset. The Kirchhoff's Current Law states that the sum of currents flowing into a node is equal to the sum of the currents flowing out of the same node. Analogously, Davies (1983) states that the algebraic sum of the wrenches belonging to the same cutset is zero. Each one of the λ components of the wrenches belonging to a subset of rigid bodies in equilibrium, defined by a cutset, must have its sum equals to zero. In order to build the system of equations to solve the statics of a mechanism, $[\hat{A}_D]_{\lambda\times C}$ is multiplied κ times by a diagonal matrix whose main diagonal is composed by the elements of each row of $[Q_A]_{\kappa\times C}$, resulting in the *network unit action matrix* $[\hat{A}_N]_{\lambda\kappa\times C}$. Multiplying this matrix by $\{\vec{\Psi}\}_{C\times 1}$, the vector containing the unknown variables of the equation system, and forcing this product to zero gives:

$$[\hat{A}_N]_{\lambda.\kappa\times C}\ \{\vec{\Psi}\}_{C\times 1} = \{\vec{0}\}_{\lambda.\kappa\times 1} \tag{7}$$

The C unknown variables related by the $\lambda.\kappa$ equations can be written as function of a subset of C_N primary variables. C_N is the *net degree of constraint* and it is determined by the difference between C and the rank a of the matrix $[\hat{A}_N]_{\lambda.\kappa\times C}$:

$$C_N = C - a \tag{8}$$

The value of C_N establishes the number of variables belonging to $\{\vec{\Psi}\}_{C\times 1}$ that must be imposed in order to solve the system of equations, i.e., to determine the values of the a secondary variables. Thus the terms of Eq. (7) can be rearranged as:

$$\{\vec{\Psi}_S\}_{a\times 1} = -[\hat{A}_{NS}]^{-1}_{a\times a}\ [\hat{A}_{NP}]_{a\times C_N}\ \{\vec{\Psi}_P\}_{C_N\times 1} \tag{9}$$

The vector $\{\vec{\Psi}\}_{C\times 1}$ is updated with the primary variables and the solution of Eq. (9) and then pre-multiplied by the unit action matrix $[\hat{A}_D]_{\lambda\times C}$, resulting in the action matrix $[A]_{\lambda\times C}$:

$$[A]_{\lambda\times C} = [\hat{A}_D]_{\lambda\times C}\ \{\vec{\Psi}\}_{C\times 1} \tag{10}$$

The condensed version of the action matrix is obtained by adding together the columns related to the same coupling, resulting in a matrix with dimensions $\lambda \times j$, where j is the number of couplings of the mechanism analysed.

2.3 Power flow and efficiency

The amount of power $\mathcal{P}$ which enters or leaves a network through a coupling e is calculated by:

$$\mathcal{P}_e = \$_e^a \cdot \$_e^m = rR + sS + tT + uU + vV + wW \tag{11}$$

The sign convention adopted herein states that if $\mathcal{P}_e < 0$, power leaves the network through coupling e, otherwise if $\mathcal{P}_e > 0$, power enters the network through coupling e.

The *overall efficiency* of a gear train is the ratio between the output and input power:

$$\eta = \frac{\mathcal{P}_{out}}{\mathcal{P}_{in}} \tag{12}$$

To estimate the *ordinary efficiency*, i.e., the efficiency of a simple gear pair, the concept of *virtual power flow* should be employed, which is the power flow measured regarding a frame that is not common to the input and output (Laus *et al.*, 2012). The virtual power flow is used to determine which gear is the driver in a gear pair, allowing to calculate the pair's efficiency. For this purpose, the carrier i is used as motion reference in the conversion of the motion matrix M in the *absolute motion matrix* M_i:

$$[M_i]_{\lambda\times n-1} = -[M]_{\lambda\times j}[I_i^\dagger]_{j\times n-1} \tag{13}$$

Where $[I_i^\dagger]_{j\times n-1}$ is the Moore-Penrose pseudoinverse of I_i, the reduced incidence matrix of the graph representing the gear train, obtained by removing the row concerning the carrier i. $[I_i^\dagger]_{j\times n-1}$ is defined by:

$$[I_i^\dagger]_{j\times n-1} = \big([I_i]_{n-1\times j}\big)^T \left([I_i]_{n-1\times j} \big([I_i]_{n-1\times j}\big)^T \right)^{-1} \tag{14}$$

The virtual power flow is calculated through the inner product between each twist in M_i and the respective wrench in A. If the result is positive, power flows in the same direction of the graph's edge, otherwise it flows in the opposite direction, defining the driver/driven relationship. The ordinary efficiency of the gear pair δ, η_δ, is computed dividing the virtual power flow that enters by the driven gear, by the one leaving from the driver gear through the gear coupling.

2.4 Loss sources as mechanical analogues of electrical resistance

Loss sources as bearing friction, seal friction and gear meshing friction can be included in the system's model by considering their effect equivalent to a pure torque when the shaft axes of the gear pair intersect (bevel gears) or are parallel (cylindrical gears) (Laus, 2011). The losses are taken into account by adding rows to $[\hat{A}_N]_{\lambda.\kappa\times C}$, generating the *augmented action matrix* D_A, the new rows being composed by the constitutive equations derived from friction models determining the magnitude of the pure torque.

Available models in the litterature include Coulomb and viscous friction. In this paper only the first one is employed, in order to quantify the gear pairs' losses. The magnitude T_δ^L of the pure torque in the Coulomb friction model is calculated by:

$$T_\delta^L = -\zeta_\delta.|U_\delta|.sign(t_\delta) = -\zeta_\delta.sign(U_\delta).sign(t_\delta).U_\delta \tag{15}$$

Where U_δ is the action transmitted by the gear pair δ, t_δ is the angular velocity of gear pair δ and ζ_δ is the coefficient of friction, in unit of length, which converts $|U_\delta|$ to a friction torque. ζ_δ is a positive value which helps to estimate the average friction torque, not the instantaneous one. However, ζ_δ can assume negative values when suposed that the power losses are not high enough to induce changes in the power flow direction, what allows to omit the absolute value operator and sign function of Eq. (15), simplifying the analysis of complex gear trains, such as automotive transmissions (Laus *et al.*, 2012). ζ_δ may be defined in function of the driver and driven gears pitch radii (r_{driver} and r_{driven}, respectively) and the ordinary efficiency of each gear pair, supposing an efficiency of $\eta_{EG} = 98\%$ for external meshing and $\eta_{IG} = 99\%$ for internal meshing (Glover, 1965). Equation (16) is intended for the former and Eq. (17), for the latter.

$$\zeta_\delta = \frac{r_{driver}r_{driven}(1-\eta_{EG})}{r_{driver}+\eta_{EG}r_{driven}} \tag{16}$$

$$\zeta_\delta = \frac{r_{driver}r_{driven}(1-\eta_{IG})}{r_{driver}-\eta_{IG}r_{driven}} \tag{17}$$

3. DHT'S STRUCTURE AND MODEL FOR SIMULATION

The DHT to be analyzed, whose schematic representation is shown in Fig. 1, consists of a simple planetary gear set and a Ravigneaux planetary gear set (Ravigneaux, 1940) in a Lepelletier configuration (Lepelletier, 1992). The EM is connected via the additional hollow ring gear of the Ravigneaux gear set. The DHT has four shift elements: one brake (B1) and three clutches (C0, C1 and C2), which enable three conventional ICE driving modes (G1, G2 and G3) that can be auxiliated by the EM in boost (e-boosting) and recuperation, and two purely electrical driving modes (E1 and E2, $E2_a$ and $E2_b$ being obtained through different clutching sequence but providing the same ratio). The transmission's shift schematic is shown in Tab. 2. This DHT has also two eCVT (electronic continuously variable transmission) driving modes, where the transmission's ratio changes seamlessly through a continuous range, however their study plus the evaluation of the e-boosting and recuperation are not in the scope of this paper. As other automotive transmissions, the system has three degrees of freedom: an ICE/EM input and the clutching sequence, which obeys the *clutch-to-clutch shift*.

In order to build a model, the DHT in Fig. 1 has its bodies numerated from 0 to 10 and the couplings connecting them are labeled from a to q. The body connecting the ICE to the link 2, called *input*, is totally determined, so it will not be included in the model. To the system has illimited rotation, all the couplings are either revolute pairs or gear pairs. From this numeration and labeling, the directed graph in Fig. 2 is built, the dashed edges representing gear pairs and the full ones, revolute pairs. The graph has seven fundamental circuits and ten fundamental cutsets, respecting the structural characteristics for epicyclic gear trains defined by Buchsbaum and Freudenstein (1970).

It must be highlighted that the planet gears 8 and 9 are connected by the gear pair p and it is considered that links 2 and 5 are united by the revolute pair i for the purpose of representing the rotation of link 5 around the central axis. Despite of the system's output being through a gearing between the ring gear 1 and some intermediary gears which lead to the vehicle's differential (Fischer, 2015), knowing the torque and angular velocity of the revolute joint j in relation to the ground link is sufficient to calculate the transmission's efficiency.

For the motion and action analyses conducted by Davies (2000) for a two-stage PGT, it was considered an order of the system $\lambda = 2$. Both revolute pairs and gear pairs, when the center distance of the two meshing gears is kept constant, allow only one independent unitary motion ($f = 1$). Consequently, for the case $\lambda = 2$, they present only one indepedendent unitary constraint $c = 1$. The following simplifying hypotheses are assumed in this paper in order to apply $\lambda = 2$:

- The DHT occupies negligible axial length, leading to all forces to lie in the plane $z = 0$ and to be parallel to the x axis. This assumption demands an adaptation of the coupling p, which passes to be a coupling connecting two spur gears whose dimensions are negligible in comparison to the others, attached to links 8 and 9, as shown in Fig. 4. Through Thales' theorem, the pitch radii r'_8 and r'_9 are defined as:

$$r'_8 = \frac{r_8(r_4+r_9-r_5-r_8)}{(r_8+r_9)}$$

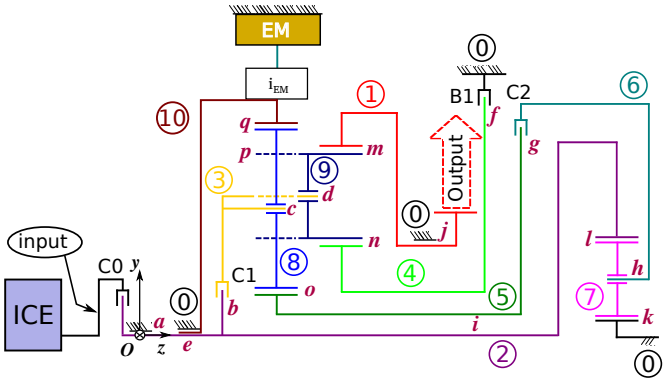

Figure 1: Schematic representation of the DHT (Adapted from (Fischer *et al.*, 2014))

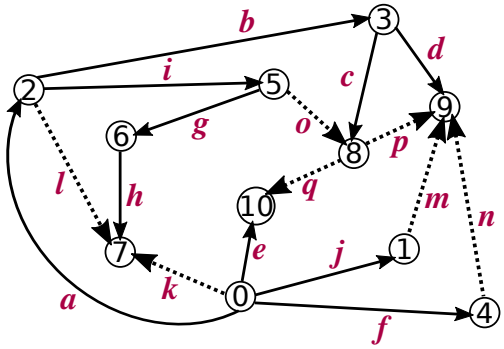

Figure 2: Graph representation of the DHT

$$r'_9 = \frac{r_9(r_4 + r_9 - r_5 - r_8)}{(r_8 + r_9)}$$

- All gears are thin spur gears whose tooth contacts lie on the y axis. Consequently, only the y coordinate of the couplings are relevant, the other elements of the vector $\vec{S}_0$ can be null. Those coordinates are defined as function of the pitch radii of the gears, shown in Fig. 3.

The vectors needed to build the twists and the wrenches through Eq. (1) and Eq. (6) are shown in Tab. 1, which contains the couplings' coordinates, the unit vectors defining the axes of the screws and the external actions acting on some couplings. The only motion allowed by all the couplings is a revolution t around the z axis, represented by the vectors $\vec{S}^M$ in the third column of Tab. 1, so the twists' pitches are $h = 0$ and the gross degree of freedom is $F = 17$. The couplings' constraints are a force U in the x direction, listed in the fourth column of Tab. 1 and whose respective wrenches have pitch $h = 0$. The couplings having an external action acting on them have an extra constraint regarding an external torque T, which may be the ICE and EM input torques, the transmission's output torque, the clutches/brake's engagement and the friction losses, as specified in the last two columns of Tab. 1 and giving wrenches with $h \to \infty$. By counting all of the constraints, the gross degree of constraint is $C = 30$.

Table 1: Couplings' coordinates, unit vectors defining the screws' axes and external actions acting on couplings

Coupling	$\vec{S}_0$	$\vec{S}^M$	$\vec{S}^A_U$	$\vec{S}^A_T$	*External action*
a	$(0,0,0)^T$	$(0,0,1)^T$	$(1,0,0)^T$	$(0,0,1)^T$	ICE input torque/Clutch C0
b	$(0,0,0)^T$	$(0,0,1)^T$	$(1,0,0)^T$	$(0,0,1)^T$	Clutch C1
c	$(0,r_5+r_8,0)^T$	$(0,0,1)^T$	$(1,0,0)^T$		
d	$(0,r_4+r_9,0)^T$	$(0,0,1)^T$	$(1,0,0)^T$		
e	$(0,0,0)^T$	$(0,0,1)^T$	$(1,0,0)^T$	$(0,0,1)^T$	EM input torque
f	$(0,0,0)^T$	$(0,0,1)^T$	$(1,0,0)^T$	$(0,0,1)^T$	Brake B1
g	$(0,0,0)^T$	$(0,0,1)^T$	$(1,0,0)^T$	$(0,0,1)^T$	Clutch C2
h	$(0,r_0+r_7,0)^T$	$(0,0,1)^T$	$(1,0,0)^T$		
i	$(0,0,0)^T$	$(0,0,1)^T$	$(1,0,0)^T$		
j	$(0,0,0)^T$	$(0,0,1)^T$	$(1,0,0)^T$	$(0,0,1)^T$	Output torque
k	$(0,r_0,0)^T$	$(0,0,1)^T$	$(1,0,0)^T$	$(0,0,1)^T$	Friction torque
l	$(0,r_0+2r_7,0)^T$	$(0,0,1)^T$	$(1,0,0)^T$	$(0,0,1)^T$	Friction torque
m	$(0,r_4+2r_9,0)^T$	$(0,0,1)^T$	$(1,0,0)^T$	$(0,0,1)^T$	Friction torque
n	$(0,r_4,0)^T$	$(0,0,1)^T$	$(1,0,0)^T$	$(0,0,1)^T$	Friction torque
o	$(0,r_5,0)^T$	$(0,0,1)^T$	$(1,0,0)^T$	$(0,0,1)^T$	Friction torque
p	$(0,r_5+r_8+r'_8,0)^T$	$(0,0,1)^T$	$(1,0,0)^T$	$(0,0,1)^T$	Friction torque
q	$(0,r_5+2r_8,0)^T$	$(0,0,1)^T$	$(1,0,0)^T$	$(0,0,1)^T$	Friction torque

Having computed the screws, the unit motion matrix $[\hat{M}_D]_{2\times17}$ and the unit action matrix $[\hat{A}_D]_{2\times30}$ are built. The vectors containing the magnitudes of the motions and the actions are:

$$\{\vec{\psi}\}_{17\times1} = \left\{ \begin{array}{ccccccccccccccccc} t_a & t_b & t_c & t_d & t_e & t_f & t_g & t_h & t_i & t_j & t_k & t_l & t_m & t_n & t_o & t_p & t_q \end{array} \right\}^T \tag{18}$$

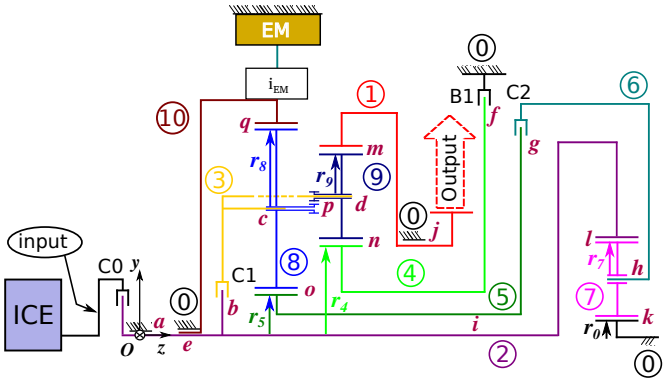

Figure 3: Pitch radii of the DHT gears

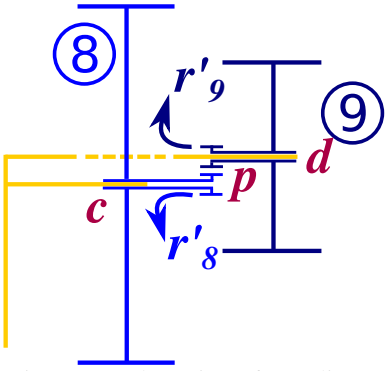

Figure 4: Adaptation of coupling p

$$\{\vec{\Psi}\}_{30\times1} = \left\{T_a\, U_a\, T_b\, U_b\, U_c\, U_d\, T_e\, U_e\, T_f\, U_f\, T_g\, U_g\, U_h\, U_i\, T_j\, U_j\, T_k\, U_k\, T_l\, U_l\, T_m\, U_m\, T_n\, U_n\, T_o\, U_o\, T_p\, U_p\, T_q\, U_q\right\}^T \quad (19)$$

The incidence matrix, the fundamental circuit matrix and the fundamental cutset matrix are shown in Eq. (20), Eq. (21) and Eq. (22), respectively:

$$[I]_{11\times17} = \begin{bmatrix}
1 & 0 & 0 & 0 & 1 & 1 & 0 & 0 & 0 & 1 & 1 & 0 & 0 & 0 & 0 & 0 & 0 \\
0 & 0 & 0 & 0 & 0 & 0 & 0 & 0 & 0 & -1 & 0 & 0 & 1 & 0 & 0 & 0 & 0 \\
-1 & 1 & 0 & 0 & 0 & 0 & 0 & 0 & 1 & 0 & 0 & 1 & 0 & 0 & 0 & 0 & 0 \\
0 & -1 & 1 & 1 & 0 & 0 & 0 & 0 & 0 & 0 & 0 & 0 & 0 & 0 & 0 & 0 & 0 \\
0 & 0 & 0 & 0 & 0 & -1 & 0 & 0 & 0 & 0 & 0 & 0 & 0 & 1 & 0 & 0 & 0 \\
0 & 0 & 0 & 0 & 0 & 0 & 1 & 0 & -1 & 0 & 0 & 0 & 0 & 0 & 1 & 0 & 0 \\
0 & 0 & 0 & 0 & 0 & 0 & -1 & 1 & 0 & 0 & 0 & 0 & 0 & 0 & 0 & 0 & 0 \\
0 & 0 & 0 & 0 & 0 & 0 & 0 & -1 & 0 & 0 & -1 & -1 & 0 & 0 & 0 & 0 & 0 \\
0 & 0 & -1 & 0 & 0 & 0 & 0 & 0 & 0 & 0 & 0 & 0 & 0 & 0 & -1 & 1 & 1 \\
0 & 0 & 0 & -1 & 0 & 0 & 0 & 0 & 0 & 0 & 0 & 0 & -1 & -1 & 0 & -1 & 0 \\
0 & 0 & 0 & 0 & -1 & 0 & 0 & 0 & 0 & 0 & 0 & 0 & 0 & 0 & 0 & 0 & -1
\end{bmatrix} \quad (20)$$

$$[B_M]_{7\times17} = \begin{bmatrix}
-1 & 0 & 0 & 0 & 0 & 0 & -1 & -1 & -1 & 0 & 1 & 0 & 0 & 0 & 0 & 0 & 0 \\
0 & 0 & 0 & 0 & 0 & 0 & -1 & -1 & -1 & 0 & 0 & 1 & 0 & 0 & 0 & 0 & 0 \\
-1 & -1 & 0 & -1 & 0 & 0 & 0 & 0 & 0 & 1 & 0 & 0 & 1 & 0 & 0 & 0 & 0 \\
-1 & -1 & 0 & -1 & 0 & 1 & 0 & 0 & 0 & 0 & 0 & 0 & 0 & 1 & 0 & 0 & 0 \\
0 & -1 & -1 & 0 & 0 & 0 & 0 & 0 & 1 & 0 & 0 & 0 & 0 & 0 & 1 & 0 & 0 \\
0 & 0 & 1 & -1 & 0 & 0 & 0 & 0 & 0 & 0 & 0 & 0 & 0 & 0 & 0 & 1 & 0 \\
1 & 1 & 1 & 0 & -1 & 0 & 0 & 0 & 0 & 0 & 0 & 0 & 0 & 0 & 0 & 0 & 1
\end{bmatrix} \quad (21)$$

$$[Q_A]_{10\times30} = \begin{bmatrix}
1 & 1 & 0 & 0 & 0 & 0 & 0 & 0 & 0 & 0 & 0 & 0 & 0 & 0 & 0 & 0 & 1 & 1 & 0 & 0 & 1 & 1 & 1 & 1 & 0 & 0 & 0 & 0 & -1 & -1 \\
0 & 0 & 1 & 1 & 0 & 0 & 0 & 0 & 0 & 0 & 0 & 0 & 0 & 0 & 0 & 0 & 0 & 0 & 1 & 1 & 1 & 1 & 1 & 1 & 0 & 0 & -1 & -1 \\
0 & 0 & 0 & 0 & 1 & 0 & 0 & 0 & 0 & 0 & 0 & 0 & 0 & 0 & 0 & 0 & 0 & 0 & 0 & 0 & 0 & 0 & 1 & 1 & -1 & -1 & -1 & -1 \\
0 & 0 & 0 & 0 & 0 & 1 & 0 & 0 & 0 & 0 & 0 & 0 & 0 & 0 & 0 & 0 & 0 & 0 & 1 & 1 & 1 & 1 & 0 & 0 & 1 & 1 & 0 & 0 \\
0 & 0 & 0 & 0 & 0 & 0 & 1 & 1 & 0 & 0 & 0 & 0 & 0 & 0 & 0 & 0 & 0 & 0 & 0 & 0 & 0 & 0 & 0 & 0 & 0 & 0 & 1 & 1 \\
0 & 0 & 0 & 0 & 0 & 0 & 0 & 0 & 1 & 1 & 0 & 0 & 0 & 0 & 0 & 0 & 0 & 0 & 0 & 0 & -1 & -1 & 0 & 0 & 0 & 0 & 0 & 0 \\
0 & 0 & 0 & 0 & 0 & 0 & 0 & 0 & 0 & 0 & 1 & 1 & 0 & 0 & 0 & 0 & 1 & 1 & 1 & 1 & 0 & 0 & 0 & 0 & 0 & 0 & 0 & 0 \\
0 & 0 & 0 & 0 & 0 & 0 & 0 & 0 & 0 & 0 & 0 & 0 & 1 & 0 & 0 & 0 & 1 & 1 & 1 & 1 & 0 & 0 & 0 & 0 & 0 & 0 & 0 & 0 \\
0 & 0 & 0 & 0 & 0 & 0 & 0 & 0 & 0 & 0 & 0 & 0 & 0 & 1 & 0 & 0 & 1 & 1 & 1 & 1 & 0 & 0 & 0 & 0 & -1 & -1 & 0 & 0 & 0 & 0 \\
0 & 0 & 0 & 0 & 0 & 0 & 0 & 0 & 0 & 0 & 0 & 0 & 0 & 1 & 1 & 0 & 0 & 0 & 0 & 0 & -1 & -1 & 0 & 0 & 0 & 0 & 0 & 0 & 0 & 0
\end{bmatrix} \quad (22)$$

$[\hat{M}_N]_{14\times17}$ and $[\hat{A}_N]_{20\times30}$ are obtained by manipulating $[B_M]_{7\times17}$ and $[Q_A]_{10\times30}$, as described in Section 2.1 and Section 2.2, respectively. The rank of the resulting $[\hat{M}_N]_{14\times17}$ is $m = 14$, giving $F_N = 3$, meaning that three velocities must be known in order to solve Eq. (2), what is expected since the system has three degrees of freedom. Those three primary variables are defined by the ICE/EM rotation and the clutching sequence, being shown in the second column of Tab. 2 for each driving mode. By contrast, the rank of $[\hat{A}_N]_{20\times30}$ is $a = 20$, resulting $C_N = 10$, therefore besides the three known actions defined by the ICE/EM input torque and the clutching sequence, shown in the last column of Tab. 2, seven constitutive equations must be included in $[\hat{A}_N]_{20\times30}$ to construct $[D_A]_{27\times30}$, culminating in the equation system $[D_A]_{27\times30}\{\vec{\Psi}\}_{30\times1} = \{\vec{0}\}_{27\times1}$.

Those constitutive equations can define the gear meshing friction losses in each one of the seven gear pairs, expressed by the simplification of Eq. (15), due to the determination of the virtual power flow direction for each gear pair through the method described in Section 2.3. Depending on the driving mode, there are some gear pairs where there is no virtual power flowing through them, which are discriminated in Tab. 3, the gear pair through which power flows being highlighted by the symbol $\triangleright$.

Table 2: Shift schematic of AVL's Future Hybrid 7 Mode (adapted from Fischer *et al.* (2014))

Driving mode	*C0*	*C1*	*C2*	*B1*	Primary variables of Motion analysis	Primary variables of Action analysis
E1		⊗	⊗		$t_b = 0, t_e = 1, t_g = 0$	$T_a = 0, T_e = 1, T_f = 0$
E2$_a$			⊗	⊗	$t_e = 1, t_f = 0, t_g = 0$	$T_a = 0, T_b = 0, T_e = 1$
E2$_b$		⊗		⊗	$t_b = 0, t_e = 1, t_f = 0$	$T_a = 0, T_e = 1, T_g = 0$
G1	⊗		⊗	⊗	$t_a = 1, t_f = 0, t_g = 0$	$T_a = 1, T_b = 0, T_e = 0$
G2	⊗	⊗	⊗		$t_a = 1, t_b = 0, t_g = 0$	$T_a = 1, T_e = 0, T_f = 0$
G3	⊗	⊗		⊗	$t_a = 1, t_b = 0, t_f = 0$	$T_a = 1, T_e = 0, T_g = 0$

Table 3: Discrimination of gear pairs through which virtual power flows, marked with ▷

Gear pair	*E1*	*E2*$_a$	*E2*$_b$	*G1*	*G2*	*G3*
k	▷			▷	▷	
l	▷			▷	▷	
m	▷	▷	▷	▷	▷	▷
n		▷	▷	▷		▷
o	▷			▷	▷	
p	▷	▷	▷	▷	▷	
q	▷	▷	▷			

The simplified expression of the Coulomb friction torque is:

$$T_\delta = \zeta_\delta . U_\delta \qquad \text{for } \delta = k, l, m, n, o, p, q \tag{23}$$

Where ζ_δ is determined by Eq. (16) in gear pairs k, n, o and p and Eq. (17) in gear pairs l, m and q. The driver/driven relationship can be verified before the inclusion of the constitutive equations, as it is assumed that the intensity of the friction torque is not enough to change the power flow direction. The equivalence $sign(\zeta_\delta) = -sign(U_\delta)sign(t_\delta)$ must be respected in order to Eq. (23) be analogous to Eq. (15). If this rule is not obeyed, the sign of ζ_δ should just be reversed.

4. EFFICIENCY CALCULATION

Having built $[\hat{M}_N]_{14\times17}$ and $[D_A]_{27\times30}$ and using the primary variables listed in Tab. 2, the motion and action analyses are solved employing Eq. (4) and Eq. (9), respectively, culminating in the motion matrix $[M]_{2\times17}$ and the condensed action matrix $[A]_{2\times17}$. The DHT's efficiency of each driving mode is calculated through Eq. (12), considering as input the power which enters the network through couplings e, $\mathcal{P}_e$, for the purely electric driving modes, and a, $\mathcal{P}_a$, for the conventional ICE driving modes, and as output the power that leaves through coupling j, $\mathcal{P}_j$:

$$\eta = -\frac{\mathcal{P}_j}{\mathcal{P}_e} \tag{24}$$

$$\eta = -\frac{\mathcal{P}_j}{\mathcal{P}_a} \tag{25}$$

The negative sign compensates the adopted sign convention. The power is calculated through Eq. (11), by the inner product between the column of $[M]_{2\times17}$ regarding the coupling whose transferable power is wished to know and its respective column of $[A]_{2\times17}$.

The values of the gears' dimensions used to obtain a numerical result are shown in Tab. 4. The overall efficiency of each driving mode is calculated by using Eq. (24) for E1 and E2 and Eq. (25) for G1, G2 and G3, the results being shown in Tab. 5.

It can be noted that among the six driving modes analyzed, the ones which present the lowest performance are E2$_a$ and E2$_b$. In spite of those two driving modes being obtained through different clutching sequences, they have the same efficiency, not existing a preference of use between them regarding the power losses. The driving mode presenting the best performance is G3, as it has less gear pairs through which power flows, the only source of losses considered in this paper, seen in the last column of Tab. 3.

Table 4: Pitch radii used in the efficiency calculation [mm]

r_0	r_4	r_5	r_7	r_8	r_9
41.8779	50.8603	43.8244	22.3903	28.9446	23.7946

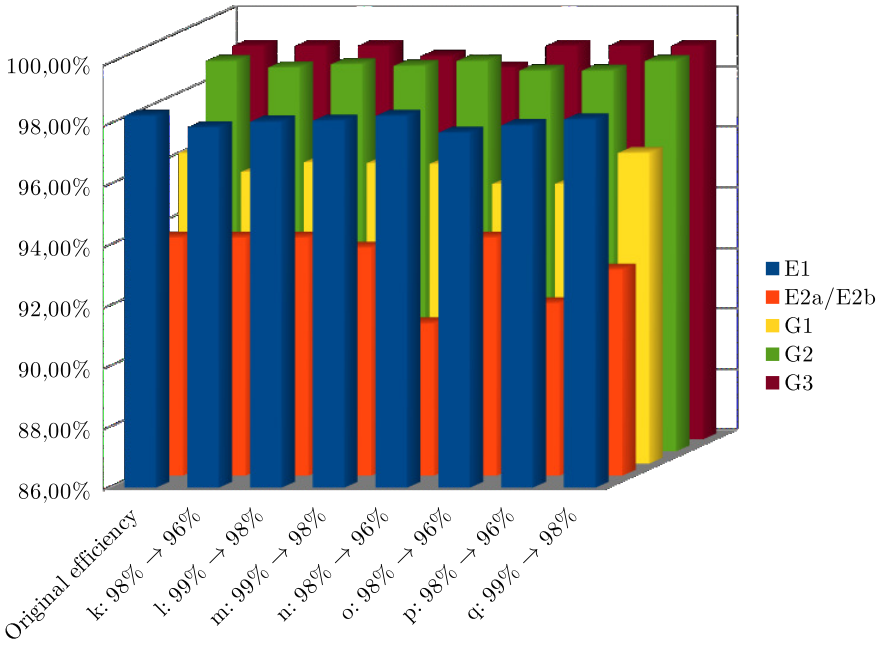

Figure 5: Sensitivity analysis of the DHT's driving modes

Table 5: Efficiency of each driving mode

E1	*E2$_a$*	*E2$_b$*	*G1*	*G2*	*G3*
98.25%	93.84%	93.84%	96.23%	98.85%	98.96%

By contrast, when the DHT is in G1, power flows through all gear pairs, except coupling q, as it is not considered the e-boosting. Consequently, G1 presents the lowest efficiency among the conventional ICE modes. Driving modes E1 and G2 are very similar, the main cause of difference of performance being the presence of power flowing through coupling q in the first, whereas this does not occur in the latter.

In an effort to identify the most sensitive driving mode to variations of friction coefficient, a sensitivity analysis was conducted, whose results are illustrated in the form of a column graph depicted in Fig. 5. The friction coefficient ζ_δ is increased by reducing the ordinary efficiency of each gear pair from 98% to 96% for external gearing and from 99% to 98% for internal gearing, then the DHT's global efficiency for a given driving mode is evaluated. Whereas the efficiency of one gear pair is decreased, the efficiency of the other ones remains the same which were used to obtain the values of Tab. 5, represented in the graph of Fig. 5 as "Original efficiency".

It is observed that the driving modes E2$_a$ and E2$_b$ are the most responsive to changes in the friction coefficient, specially when they occur in couplings n and p. Although not so intense, the efficiency of coupling q has also some impact on the global effcency of the DHT when E2$_a$ or E2$_b$ are engaged. G1 presents a certain sensitivity as well to alterations in the friction coefficient of couplings o and p, though not so significant. The other driving modes do not manifest any meaningful reduction in the overall performance. Consequently, the most critical couplings are n, o and p with respect to E2$_a$, E2$_b$ and G1's efficiency.

5. CONCLUSIONS

The study of automotive transmission's efficiency is an important step towards the consumption and emissions reduction. This paper presented an application of the method to calculate gear trains' efficiency developed by Laus (2011) in a transmission category in vogue: the Dedicated Hybrid Transmission. By doing an electromechanical analogy through graph and screw theories, where the loss sources are considered analogues of the electrical resistance, the efficiency of complex automotive transmissions is easily estimated for each driving mode.

The next steps comprehend not only the determination of the eCVT driving modes' performance and the verification of the impact of the e-boosting on the conventional ICE driving modes, but also the inclusion of viscous friction models in the revolute pairs to take into account bearing losses in the overall efficiency calculation. Moreover, an optimization process can be applied in order to determine the gears' dimensions that assure the maximum efficiency of the driving mode which is the most demanded in specific circunstances, such as urban traffic, where the request of the first ratios is stronger, or highway traffic, where the last ratios are more required.

6. ACKNOWLEDGEMENTS

Thanks are due to CNPq for financial support.

7. REFERENCES

Buchsbaum, F. and Freudenstein, F., 1970. "Synthesis of kinematic structure of geared kinematic chains and other mechanisms". *Journal of mechanisms*, Vol. 5, No. 3, pp. 357–392.

Cazangi, H.R., 2008. *Aplicação do método de Davies para análise cinemática e estática de mecanismos com múltiplos graus de liberdade*. Master's thesis, Universidade Federal de Santa Catarina.

Changenet, C., Oviedo-Marlot, X. and Velex, P., 2006. "Power loss predictions in geared transmissions using thermal networks-applications to a six-speed manual gearbox". *Journal of Mechanical Design*, Vol. 128, No. 3, pp. 618–625.

Davies, T., 1981. "Kirchhoff's circulation law applied to multi-loop kinematic chains". *Mechanism and machine theory*, Vol. 16, No. 3, pp. 171–183.

Davies, T., 1983. "Mechanical networks iii - wrenches on circuit screws". *Mechanism and Machine Theory*, Vol. 18, No. 2, pp. 107–112.

Davies, T., 2000. "The 1887 committee meets again. subject: freedom and constraint". In *Proceedings of a Symposium commemorating the legacy, works and life of Sir Robert Stawell Ball upon the 100th Anniversary of 'A Treatise on the theory of Screws'*.

Fischer, R., 2015. "Dedicated hybrid transmissions (dht)". *CTI Mag*, , No. 5, pp. 6–8.

Fischer, R., Beste, F. and Yolga, M., 2014. "Seven-mode transmission for plug-in hybrid concepts". *MTZ worldwide*, Vol. 75, No. 12, pp. 10–17.

Glover, J.H., 1965. "Efficiency and speed-ratio formulas for planetary gear systems". *Prod. Eng.(NY)*, Vol. 27, pp. 72–79.

Hsieh, H.I. and Tsai, L.W., 1998. "The selection of a most efficient clutching sequence associated with automatic transmission mechanisms". *Journal of mechanical design*, Vol. 120, No. 4, pp. 514–519.

Irimescu, A., Mihon, L. and Pădure, G., 2011. "Automotive transmission efficiency measurement using a chassis dynamometer". *International Journal of Automotive Technology*, Vol. 12, No. 4, pp. 555–559.

Laus, L., Simas, H. and Martins, D., 2012. "Efficiency of gear trains determined using graph and screw theories". *Mechanism and Machine Theory*, Vol. 52, pp. 296–325.

Laus, L.P., 2011. *Determinação da eficiência de máquinas com base em teoria de helicoides e grafos: aplicaÃğção em trens de engrenagens e robôs paralelos*. Ph.D. thesis, Universidade Federal de Santa Catarina.

Lepelletier, P.A., 1992. "Multispeed automatic transmission for automobile vehicles". US Patent 5,106,352.

Mantriota, G., 2002. "Performances of a series infinitely variable transmission with type i power flow". *Mechanism and Machine Theory*, Vol. 37, No. 6, pp. 579–597.

Moskalik, A., Hula, A., Barba, D. and Kargul, J., 2016. "Investigating the effect of advanced automatic transmissions on fuel consumption using vehicle testing and modeling". *SAE International Journal of Engines*, Vol. 9, No. 2016-01-1142, pp. 1916–1928.

Ravigneaux, P., 1940. "Speed changing device". US Patent 2,220,174.

8. RESPONSIBILITY NOTICE

The authors are the only responsible for the printed material included in this paper.